



## Combined conductive and radiative heat transfer in an anisotropic scattering participating medium with irregular geometries

H. Amiri <sup>a,\*</sup>, S.H. Mansouri <sup>a</sup>, A. Safavinejad <sup>b</sup>

<sup>a</sup>Department of Mechanical Engineering, Shahid Bahonar University of Kerman, Kerman, Iran

<sup>b</sup>Department of Mechanical Engineering, Birjand University, Birjand, Iran

### ARTICLE INFO

#### Article history:

Received 29 April 2009

Received in revised form

15 October 2009

Accepted 16 October 2009

Available online 3 November 2009

#### Keywords:

Blocked-off method

Finite volume method

Irregular geometries

Discrete ordinate method

Conduction

Radiation

### ABSTRACT

This paper deals with the numerical solution for the steady state combined conductive–radiative heat transfer in an anisotropic participating medium within the irregular geometries using the blocked-off method in Cartesian coordinates. The walls of the enclosures were considered to be opaque, diffuse and gray having specified heat flux and temperature boundary conditions. The finite-volume method has been adopted to solve the energy equation and the discrete ordinates method has been employed to solve the radiative transfer equation. The radiative and radiative–conductive models were validated by comparison with the results of specific test cases taken from the literature. The results showed very satisfactory predictions compared with the benchmarked results. As the degree of enclosure complexity (with curved or skewed walls) increased, finer grids were required. Based on this method, the effects of various influencing parameters such as the conduction–radiation parameter, scattering albedo and extinction coefficient have been considered.

© 2009 Elsevier Masson SAS. All rights reserved.

### 1. Introduction

The problem of radiation coupled with other modes of heat transfer is encountered in many engineering applications. The combined conductive–radiative heat transfer has numerous engineering applications such as heat transfer through the semi-transparent, porous materials, multilayered insulations, glass fabrication, industrial furnaces, optical textile fiber processing, fibrous insulation, and etc. The constitutive medium in the majority of these systems actively participates in the radiative transfer due to the absorption, emission and scattering of radiation.

Several numerical methods have been developed for the radiative heat transfer problems, including the Zonal method, the Monte Carlo method, the spherical harmonics method, the Discrete Transfer Method (DTM), the Discrete Ordinates Method (DOM), the Finite-Volume Method (FVM), the Finite Element Method (FEM), and the Ray-Tracing/Nodal-Analyzing Method (RTNAM), all of which except the RTNAM are classical and well known. Therefore, the advantages and disadvantages of these methods are not mentioned here. The RTNAM was first proposed by Tan and Lallemand [6] and has recently been developed by several researchers

[7–9]. Its advantage is that the radiative intensity does not need to be dispersed along the space coordinate when solving the radiative transfer equation and the solid angle is not dispersed but is directly integrated. Thus, the false scattering and the ray effect will not exist in this method. Therefore, the theoretical accuracy of this method is high. The disadvantage of this method is that it is very difficult to solve the radiative heat transfer in a multi-dimensional medium.

Although the Zonal and the Monte Carlo methods are often considered as the most accurate ones, these methods have great difficulties in treating the combined mode of heat transfer and their computational requirements. Hence, none of the methods currently available can be considered as the best one for all the problems. Among the other methods, the discrete ordinates method has received an increasingly high attention because of its efficient integration with different methods of solving the energy equation such as FVM and FEM. This method is a simplified, but attractive, method to solve the radiative transfer problems and provides a good compromise between the accuracy and the computational economy. This method was originally formulated by Chandrasekhar [10] and developed by Lathrop and Carlson [11] and Lathrop [12]. Fiveland [13,14] presented the general outlines of the method and formulated an accurate method of discrete ordinates of the first order based on the method of finite volumes for two-dimensional and three-dimensional enclosures. Ramankutty and Crosbie [15,16] presented a more recent and extensive review of the DOM and used this method to formulate the so-called modified discrete ordinates

\* Corresponding author.

E-mail addresses: [sf\\_tb2003@yahoo.com](mailto:sf_tb2003@yahoo.com) (H. Amiri), [mansouri@alum.mit.edu](mailto:mansouri@alum.mit.edu) (S.H. Mansouri), [a\\_safavinejad@yahoo.com](mailto:a_safavinejad@yahoo.com) (A. Safavinejad).

Nomenclature	
$A_x, A_y$	areas of the control-volume faces normal to the $x$ and $y$ directions ( $\text{m}^2$ )
$a_0$	asymmetry factor
$F, F_x, F_y$	blocked-off variables in center, $x$ and $y$ direction
$G$	incident radiation ( $\text{W m}^{-2}$ )
$G^*$	dimensionless incident radiation
$k$	thermal conductivity ( $\text{W m}^{-1} \text{K}^{-1}$ )
$M$	number of discrete directions
$n$	refractive index
$\vec{n}_w$	outward unit vector normal to the wall
$N$	number of different direction cosines
$N_{CR}$	conduction–radiation parameter
$I_b$	black body radiation intensity ( $\text{W m}^{-2}$ )
$I$	radiation intensity ( $\text{W m}^{-2}$ )
$I_{ij}^m$	intensity at grid node $i, j$ and in $m$ direction ( $\text{W m}^{-2}$ )
$Q$	dimensionless heat flux value
$\vec{q}_R$	radiative heat flux vector ( $\text{W m}^{-2}$ )
$\vec{r}_{w-T}$	temperature specified part of boundary
$\vec{r}_{w-F}$	heat flux specified part of boundary
$\vec{s}$	geometric path vector
$S_{ij}^m$	source term
$S_C, S_P$	constant of linearization of energy source term
$T$	absolute temperature (K)
$T_{ref}$	reference temperature (K)
$V$	volume ( $\text{m}^3$ )
$w$	weight of angular quadrature
$x, y$	$x, y$ coordinates
$X, Y$	dimensionless coordinates
<i>Greek symbols</i>	
$\beta$	extinction coefficient ( $\text{m}^{-1}$ )
$\omega$	scattering albedo
$\eta$	fraction of radiation to total heat flux
$\varepsilon_w$	wall emissivity
$\sigma_s$	scattering coefficient ( $\text{m}^{-1}$ )
$\mu^m, \xi^m$	$x$ and $y$ cosines of $\vec{s}^m$ direction
$\gamma_x, \gamma_y$	spatial differencing weights to $x$ and $y$ directions
$\varphi$	scattering phase function
$\kappa$	absorption coefficient ( $\text{m}^{-1}$ )
$\theta$	dimensionless temperature
$\sigma$	Stefan–Boltzmann constant ( $\text{W m}^{-2} \text{K}^{-4}$ )
$\Omega$	solid angle (sr)
$\Gamma$	tolerance
<i>Superscripts</i>	
$*$	dimensionless variable
<i>Subscripts</i>	
$in$	upstream
$CR$	conduction–radiation
$R, C, T$	radiation, conduction and total
$out$	downstream
$ref$	reference
$w$	wall

method. Sakami and Charette [17] applied the modified discrete ordinates method to two-dimensional enclosures of the irregular geometries.

Solving the radiative transfer equation (RTE) and its applicability to the irregular multi-dimensional problems is always a challenging task. The irregular geometries may be modeled simply using the non-orthogonal grids. However, it is desirable to formulate a solution procedure to model the irregular geometries using Cartesian coordinates formulations in order to avoid additional complexities arising from the non-orthogonality of the computational grids. Sanchez and Smith [1] discussed the radiative exchange of a square geometry with a square obstacle in the middle using the discrete ordinates method for a non-participating media. In the participating media, Chai et al. [2,3] discussed different possibilities of solving the radiative transfer problems in the irregular structures using the discrete ordinates method, the finite-volume method and the Monte Carlo method. They implemented the blocked-off procedures in the discrete ordinates method [2] and the finite-volume method [3] for different kinds of irregular structures.

Byun et al. [4] investigated the radiative heat transfer in the complex geometries using blocked-off, multiblock, and embedded boundary treatments. Asllanaj et al. [5] proposed a new Finite-Volume Method (FVM) based on a cell vertex scheme, associated to a new modified exponential scheme to solve the radiative heat transfer problem in 2-D irregular geometries containing absorbing, emitting and non-scattering gray media.

Many researchers studied the two-dimensional coupled radiative and conductive heat transfers in a participating medium. In rectangular enclosures, Yuen and Takara [18] solved the radiation problem using a generalized exponential integral function and the coupled problem by one empirical additive approach. Also, Kim and Baek [19] solved the same problem using the DOM with diamond

spatial scheme for the radiative part of the problem while the conductive term was discretized using the central difference scheme. Lee and Viskanta [20] compared the solutions of the combined conductive–radiative heat transfer in the two-dimensional semitransparent media using the finite-volume method for the energy equation coupled with the DOM and diffusion approximations for the RTE. Mishra et al. [21] solved the transient conductive and radiative heat transfer in a two-dimensional rectangular enclosure filled with an absorbing, emitting and scattering medium. The radiative transfer equation was solved by the collapse dimension method while the energy equation was alternatively solved by the Lattice Boltzmann Method (LBM) and the FVM; the performance and the computational cost of the LBM and the FVM were compared.

Mahapatra and Mahapatra [22] studied coupled radiative and conductive heat transfer in an isotropic scattering square enclosure using the DOM. The enclosure comprised isothermal vertical walls and insulated horizontal walls. Later, Mahapatra et al. [23] numerically solved the same problem by the development of a hybrid method combining the spherical harmonics method and the DOM. The industrial heat transfer problems at elevated temperatures, such as burners, kilns, boilers and combustion chambers, etc., always deal with the irregular geometries and the radiative heat transfer plays a predominant role in these industrial applications. The combined conductive and radiative heat transfer in the irregular geometries has been studied by some researchers. Sakami et al. [24] used a modified discrete ordinates method based on the incorporation of directional ray propagation relations within the cells with triangular grids and they used the finite element technique in the conduction part of the coupled problem. Rousse [25] and Rousse et al. [26] used the finite-volume method for solving the RTE and the finite element method for solving the energy equation in the solution of conduction–radiation and convection–radiation problems in two-dimensional cavities and canals.

Ismail and Salinas [27] used the discrete ordinates method with a multi-dimensional spatial scheme for the radiative part and used the finite-volume method for solving the energy equation. Asllanaj et al. [28] solved the transient radiation and conduction heat transfer in a gray absorbing-emitting medium in a two-dimensional complex-shaped domain using the unstructured triangular meshes. The RTE was solved by using a new FVM based on a cell vertex scheme and associated to a modified exponential scheme. Luo and Shen [29] used the ray tracing-node analyzing method to solve a 2-dimensional transient coupled heat transfer in a rectangular semi-transparent medium. The transient energy equation is discretized using the fully implicit finite difference method and the radiative source term is expressed using the radiative transfer coefficients.

A limited number of research works have been carried out to analyze the coupled conductive and radiative heat transfer within the multi-dimensional irregular geometries with the blocked-off procedure and in almost all of which, the combined conduction and radiation heat transfer problems have been solved within the enclosures comprised of isothermal walls. Moreover, most of the previous works on the radiative heat transfer considered only isotropic scattering or non-scattering in the semitransparent medium.

Here, we present a solution procedure for the combined conductive–radiative heat transfer problem in the irregular geometries having gray diffusive walls; containing gray, absorbing, emitting anisotropic scattering medium using the blocked-off finite-volume method in Cartesian coordinates. The walls of the enclosures can have either the specified heat flux boundary conditions or the specified temperature boundary conditions. The energy equation is solved using the FVM taking the divergence of the radiative heat flux vector as the source term. The RTE is solved by the discrete ordinate method. The predicted results are validated with the results obtained from the literature and the effects of the main thermophysical parameters on the temperature and heat flux values are demonstrated.

## 2. Problem formulation

The steady state conservation of energy equation in the absence of convection and heat generation is expressed as:

$$k \left( \frac{\partial^2 T}{\partial x^2} + \frac{\partial^2 T}{\partial y^2} \right) - \nabla \cdot \vec{q}_R = 0 \quad (1)$$

assuming constant properties in the two-dimensional Cartesian coordinates system. Where  $k$  is the thermal conductivity and  $\nabla \cdot \vec{q}_R$  is the divergence of the radiative heat flux given by

$$\nabla \cdot \vec{q}_R = \kappa \left( 4\pi I_b(T(\vec{r})) - \int_{4\pi} I(\vec{r}, \vec{s}) d\Omega \right) \quad (2)$$

where,  $\kappa$  is the absorption coefficient,  $I(\vec{r}, \vec{s})$  is the radiation intensity at the position  $\vec{r}$  and in the direction  $\vec{s}$ ,  $I_b(T(\vec{r})) = n^2 \sigma(T(\vec{r}))^4 / \pi$  is the black body radiation intensity and  $n$  is the refractive index of the medium and is equal to one in this study.

To obtain the radiation intensity field and  $\nabla \cdot \vec{q}_R$ , it is necessary to solve the RTE. The RTE for an absorbing, emitting and scattering gray medium can be written as ([30])

$$(\vec{s} \cdot \nabla) I(\vec{r}, \vec{s}) = -\beta I(\vec{r}, \vec{s}) + \kappa I_b(\vec{r}) + \frac{\sigma_s}{4\pi} \int_{4\pi} I(\vec{r}, \vec{s}') \varphi(\vec{s}' \rightarrow \vec{s}) d\Omega' \quad (3)$$

in which  $\sigma_s$  is the scattering coefficient,  $\beta = \kappa + \sigma_s$  is the extinction coefficient and  $\varphi(\vec{s}' \rightarrow \vec{s})$  is the scattering phase function for the radiation from incoming direction  $\vec{s}'$  and confined within the solid

angle  $d\Omega'$  to scattered direction  $\vec{s}$  confined within the solid angle  $d\Omega$ . In this paper, linear-anisotropic scattering is considered, in which the phase function for linear-anisotropic scattering is:

$$\varphi(\vec{s}' \rightarrow \vec{s}) = 1.0 + a_0(\vec{s}' \cdot \vec{s}) \quad (4)$$

where  $-1 \leq a_0 \leq 1$  is an asymmetry factor. Values of the parameter  $a_0$  are  $+1$ ,  $0$  or  $-1$  whether the scattering is forward, isotropic or backward, respectively.

The boundary condition for a diffusely emitting and reflecting gray wall is

$$I(\vec{r}_w, \vec{s}) = \varepsilon_w I_b(\vec{r}_w) + \frac{(1 - \varepsilon_w)}{\pi} \int_{\vec{n}_w \cdot \vec{s}' < 0} I(\vec{r}_w, \vec{s}') \times |\vec{n}_w \cdot \vec{s}'| d\Omega', \quad \vec{n}_w \cdot \vec{s} > 0 \quad (5)$$

where,  $\varepsilon_w$  is the wall emissivity,  $I_b(T(\vec{r}_w))$  is the black body radiation intensity at the temperature of the boundary surface and  $\vec{n}_w$  is the outward unit vector normal to the surface. Since the radiative transfer equation depends on the temperature field through the emission term ( $I_b(T(\vec{r}))$ ) thus it must be solved simultaneously with the overall energy equation. Here, the discrete ordinates method is used to solve the RTE.

## 3. Numerical method

In the discrete ordinates method, the radiative transfer equation is changed by a discrete set of  $M$  coupled differential equations for a finite number of directions  $\vec{s}^m (m = 1, 2, \dots, M)$ . Integrals over the solid angles are changed by a quadrature of order  $M$ , yielding

$$(\vec{s}^m \cdot \nabla) I(\vec{r}, \vec{s}^m) = -\beta I(\vec{r}, \vec{s}^m) + \kappa I_b(\vec{r})$$

$$+ \frac{\sigma_s}{4\pi} \sum_{n=1}^M I(\vec{r}, \vec{s}^n) \varphi(\vec{s}^n \rightarrow \vec{s}^m) w^n \quad (6)$$

in which  $w^n$  is the quadrature weight of the direction  $\vec{s}^n$ . In the present work, the level symmetric quadratures,  $S_N$ , have been used where  $M = N(N + 2)$ . In discrete ordinates, the boundary condition expressed by Equation (5) is discretized as

$$I(\vec{r}_w, \vec{s}^m) = \varepsilon_w I_b(\vec{r}_w) + \frac{(1 - \varepsilon_w)}{\pi} \sum_{n=1, \vec{n}_w \cdot \vec{s}^n < 0}^M I(\vec{r}_w, \vec{s}^n) \times |\vec{n}_w \cdot \vec{s}^n| w^n, \quad \vec{n}_w \cdot \vec{s}^m > 0 \quad (7)$$

and the divergence of the radiative heat flux is expressed as

$$\nabla \cdot \vec{q}_R = \kappa \left( 4\pi I_b(\vec{r}) - \sum_{n=1}^M I(\vec{r}, \vec{s}^n) w^n \right) \quad (8)$$

Spatial discretization of the discrete ordinates equations is carried out using the finite-volume approach. Equation (6) is integrated using the Gauss divergence theorem over a typical control volume (Fig. 1) in which the right-hand side of Equation (6) is assumed to be constant over the control volume. For a two-dimensional Cartesian coordinates system and for a direction  $\vec{s}^m$  with direction cosines  $\mu^m$  and  $\xi^m$ , integrating yields the discretized equation

$$|\mu^m| A_x (I_{x,out}^m - I_{x,in}^m) + |\xi^m| A_y (I_{y,out}^m - I_{y,in}^m) = (-\beta I_{i,j}^m + S_{i,j}^m) V \quad (9)$$

where,

$$S_{i,j}^m = \kappa I_b \cdot i,j + \frac{\sigma_s}{4\pi} \sum_{n=1}^M I_{i,j}^n \varphi(\vec{s}^n \rightarrow \vec{s}^m) w^n \quad (10)$$

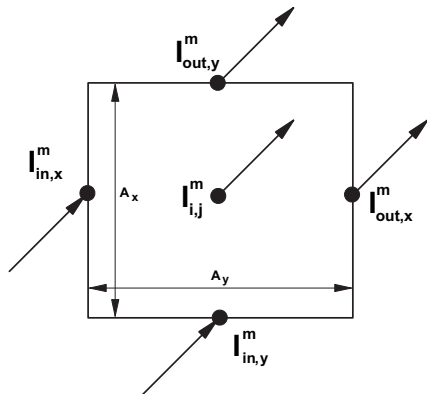


Fig. 1. A typical control volume.

in which,  $I_{i,j}^m$  is the intensity at the grid node  $(i,j)$  and in direction  $\vec{s}^m$ . The subscripts of the cell face intensities represent the direction ( $x$  or  $y$ ) and the upstream ( $in$ ) or downstream ( $out$ ) through the face. The radiation intensities at the cell faces are unknown and must be related to the radiation intensities at the neighboring grid nodes. Most often a linear relationship is chosen as:

$$I_{i,j}^m = \gamma_x I_{x,out}^m + (1 - \gamma_x) I_{x,in}^m = \gamma_y I_{y,out}^m + (1 - \gamma_y) I_{y,in}^m \quad (11)$$

in which  $\gamma_x$  and  $\gamma_y$  are the spatial differencing weights to the  $x$  and  $y$  directions, respectively. The standard diamond difference scheme ( $\gamma_x = \gamma_y = 0.5$ ) which is commonly used and has a good accuracy, is unstable and gives oscillatory and negative intensity solutions especially when there is a significant difference between the radiation intensities on adjacent faces of the control volume for the treatment of the blocked-off irregular geometries [31]. Therefore, we choose the step scheme ( $\gamma_x = \gamma_y = 1.0$ ) which is simple, convenient, stable and ensures positive intensities. The final discretized equation for a nodal point  $i,j$  can be obtained by applying the spatial differencing equation to Equation (9) as follows

$$I_{i,j}^m = \frac{|\mu^m| A_x I_{x,in}^m + |\xi^m| A_y I_{y,in}^m + S_{i,j}^m V}{|\mu^m| A_x + |\xi^m| A_y + \beta V} \quad (12)$$

The numerical solution of Equation (12) is described in [13,14,30].

To solve the coupled radiation–conduction problem, the energy equation is converted to a non-dimensional form, presented in Appendix A.

#### 4. Blocked-off method

In order to avoid the complexity of treating the non-orthogonal grids, it is suitable to formulate a procedure to model the irregular geometries using the Cartesian coordinates. The combined conductive and radiative heat transfer in the irregular geometries is modeled using the blocked-off method commonly used in the CFD. The blocked-off procedure consists of drawing rectangular nominal domains around the given physical domains (Fig. 2). The new domain contains active and inactive regions. The active regions, where the solutions are sought, are unshaded in Fig. 2(b). The shaded regions outside the real domain are called the inactive or the blocked-off regions, where the solutions are not meaningful and thus are not sought and are retained to form the nominal domain. In the geometries with inclined and curved boundaries, the boundaries are approximated with ladder-like lines as shown in Fig. 2(d). This enables the modeling of irregular geometries with

computer programs in Cartesian coordinates. For the inclined or curved irregular geometries, a relatively fine grid can produce reasonably accurate solutions.

This procedure has been developed for the conductive and convective heat transfer by Patankar [32]. Then, it was extended to the two-dimensional radiative transfer problem by Chai [2,3]. Here, we use the two-dimensional formulation of the block-off method for the combined conductive–radiative heat transfer. In order to distinguish active cells from inactive ones in the standard blocked-off method, an additional source term is introduced in the energy and radiative transfer equations ([2,3,32]).

In the present study, we use a new form of the blocked-off method in which three blocked-off variables are defined instead of introducing an additional source term for each control volume. Fig. 2(c) shows how a domain is described in this new form of the blocked-off method. The whole nominal domain is discretized into several control volumes. Then, for each control volume  $(i,j)$ , five variables, namely the blocked-off variables, have been defined. One of them is assigned to the center of the control volume denoted as  $F(i,j)$  and the others are assigned to the  $x$  and  $y$  sides of the control volume denoted as  $F_x(i-1,j-1)$ ,  $F_x(i,j-1)$ ,  $F_y(i-1,j-1)$  and  $F_y(i-1,j)$  (Fig. 2(c)). Indeed, the blocked-off variables only take values 0 or 1. If the center of the control volume is in the inactive region, the blocked-off variables take the value 1 and otherwise they take 0. Also, the blocked-off variables of the side walls of the control volume which coincide with the nominal domain take the value 1. Fig. 2(d) shows the values of the blocked-off variables in the nominal geometry for a coarse grid. In the numerical methods section we explain how this variable is used.

The energy equation which is nonlinear is discretized using the finite-volume method as in Patankar [32]. It is worth noting that not only the governing transport equations are coupled, but also their boundary conditions are interlocked. Thus, an iterative solution is needed.

One can identify the energy equation, as the Fourier conduction equation with a radiative source term. As the radiative source term has a strong nonlinearity in the non-dimensional temperature,  $\theta$ , the source term in Equation (A2) is linearized using Taylor series expansion around the value of the previous iteration as

$$-\theta_p^4 = S_C + S_p \theta_p^k \quad (13)$$

where  $S_C = 3(\theta_p^{k-1})^4$ ,  $S_p = -4(\theta_p^{k-1})^3$ , and  $k$  and  $k-1$  denote the current and previous iteration value of the parameters, respectively.

The procedure of the numerical calculations is as follows:

1. Assume the temperature distributions over the entire medium and the boundary surfaces with specified heat flux boundary condition.
2. Solve the RTE using the DOM method for all control volumes and all directions as follows: For each direction  $m$  and for each control volume  $(i,j)$  the radiation intensity is calculated by the following algorithm:
  - a) For each control volume  $(i,j)$  that  $F(i,j) = 1$ , if the side wall of the blocked-off variable have the value of 1, then, the upstream radiation intensity is calculated by Equation (7) otherwise they were previously calculated from Equation (11) in the current or previous iteration.
  - b) Having the upstream radiation intensity,  $I_{x,in}^m$  and  $I_{y,in}^m$ , the control-volume radiation intensity,  $I_{i,j}^m$ , is calculated by Equation (12).
  - c) The downstream radiation intensity is calculated using equation (11).
3. Calculate the divergence of the radiative heat flux for the active region.

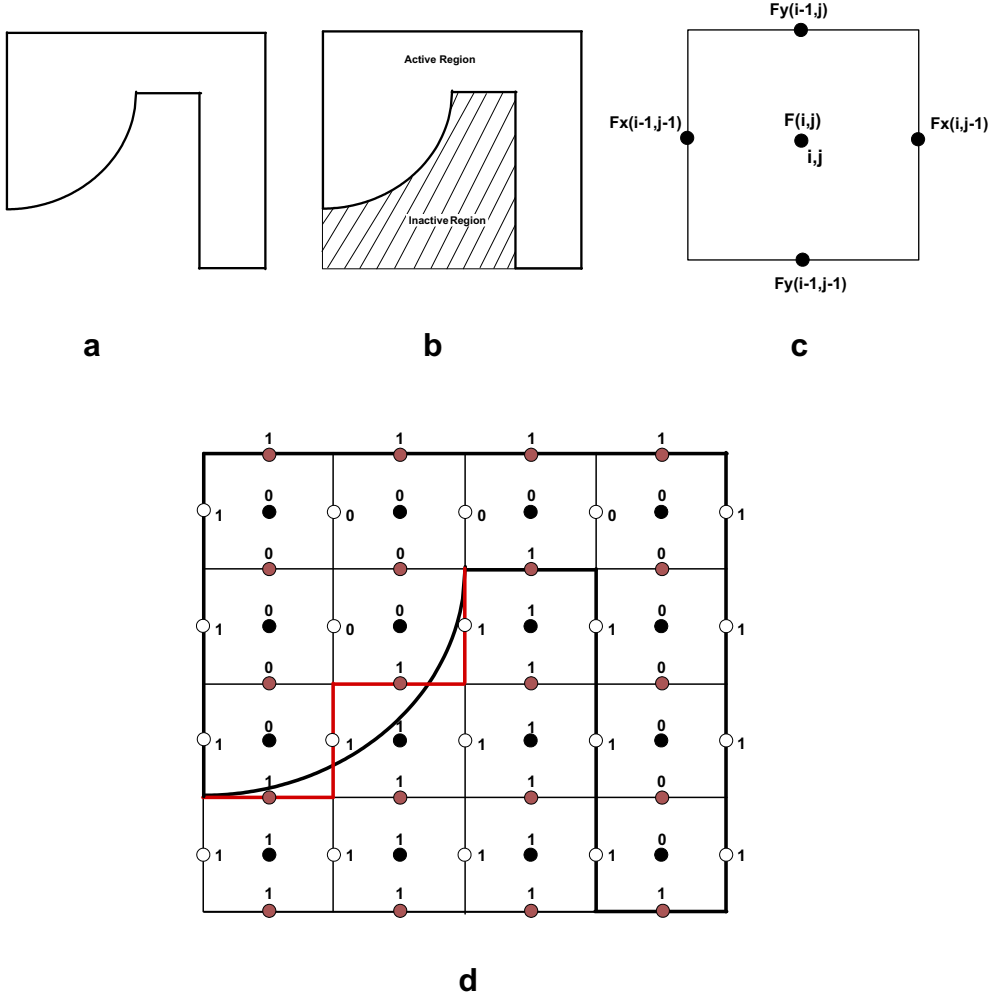


**Fig. 2.** (a) Real geometry, (b) nominal geometry, (c) blocked-off variables definition, (d) value of blocked-off variables in nominal geometry (colors show central (black), x-side (white) and y-side (brown) block-off variables). (For interpretation of the references to color in this figure legend, the reader is referred to the web version of this article.)

4. Solve the energy equation for the active region to obtain the temperature  $\theta_{i,j}^k$  in the medium and walls with the specified heat flux boundaries.
5. Repeat steps 2–4 until  $\text{Max} \left( \frac{|\theta_{i,j}^k - \theta_{i,j}^{k-1}|}{\theta_{i,j}^{k-1}} \right) < \Gamma$ .

The prescribed tolerance ( $\Gamma$ ) is set to  $10^{-8}$  in this study.

## 5. Validation procedure

We have tested the validity of the combined conductive–radiative heat transfer for a simple geometry for which exact or reliable solutions is available. Then, we have tested the blocked-off method for the case of radiative heat transfer in an irregular geometry before applying the new method to enclosures of the irregular geometries with combined conductive–radiative heat transfer. In this study, the heat fluxes are non-dimensionalized by dividing them by  $\sigma T_{ref}^4$  in which  $T_{ref}$  is the maximum temperature in the enclosure.

## 6. Validation of the combined conductive–radiative heat transfer

Consider the combined conductive–radiative heat transfer in an enclosure of infinite length with a square cross-section containing

an absorbing, emitting, non-scattering medium ( $\omega = 0$ ), in which the enclosure is in radiative equilibrium and has black walls. The left wall ( $X = 0$ ) is at the dimensionless temperature of  $\theta_b = 1$  and the other walls are at the temperature  $\theta_{other} = 0.5$ . This problem was solved by Yuen et al. [18], Kim and Baek [19], Ismail and Salinas [27] and Sakami et al. [24]. For validation, we compared our results with the results of Ismail and Salinas [27] and Sakami et al. [24].

Fig. 3(a) shows the dimensionless temperature profiles along the symmetry line ( $Y = 0.5$ ) for three angular quadratures and  $N_{CR} = 0.01$ . Here we use a uniform spatial grid of  $N_x \times N_y = 21 \times 21$ . The results, compared with those of Refs. [24, 27] show good agreement for all the quadratures. The profile for  $S_4$  is very close to the result of Ref. [24] with the same quadrature. Using a higher quadrature, the profile converges to the results of Ref. [27] with LC11 quadrature. The results show that  $S_8$  angular quadrature gives satisfying results. Fig. 3(b) shows the temperature distribution in the medium for the two conduction–radiation parameters. The results show good agreement with those of Sakami et al. [24] and Ismail and Salinas [27].

Another test was done for the same problem shown in Fig. 4 in which the dimensionless total heat flux (radiative and conductive) on the hot face is given versus the vertical position for  $N_{CR} = 0.01$ . Again, the results show good agreement with respect to those of Ismail and Salinas and Sakami et al. As  $N_{CR}$  decreases, the role of the

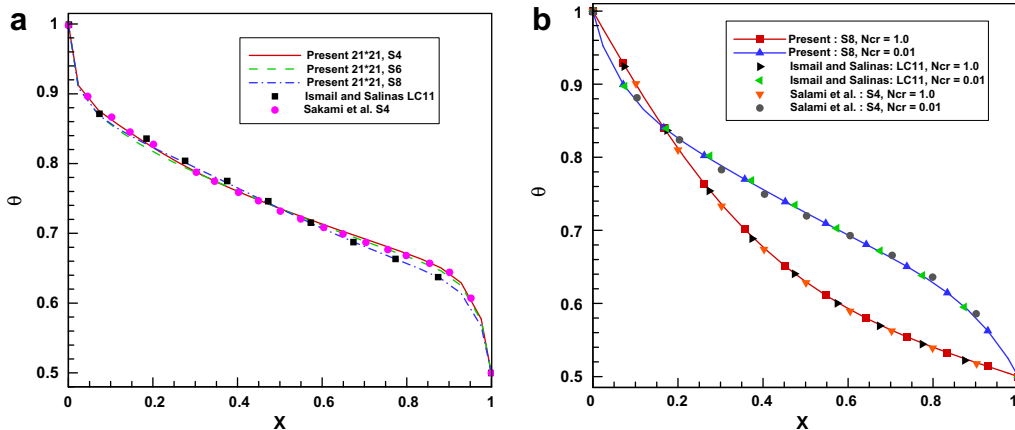


Fig. 3. (a) Comparison of solution convergence for different angular quadratures. (b) Comparison of the distribution of the non-dimensional temperatures in the medium along the symmetry line ( $Y = 0.5$ ) for two conduction–radiation parameters.

radiation increases and the energy is transmitted deeper into the medium, producing higher temperature gradients at both faces and increasing the temperatures near the cold face.

## 7. Validation of the blocked-off method

To check the performance and accuracy of the present method, the blocked-off boundary treatment is applied to a semicircular enclosure with an inner circle containing an absorbing, emitting and non-scattering medium with  $\beta = 1 \text{ m}^{-1}$  (Fig. 5). It is assumed that the thermal conductivity of the medium is zero ( $k = 0$ ). The medium is enclosed by the semicircle and the inner circle is maintained at a constant temperature of 1000 K. The enclosure walls are assumed to be cold and black. The spatial grid and ordinate system used here is  $N_x \times N_y = 100 \times 50$  and  $S_{10}$ , respectively. A comparison of the non-dimensional radiative heat flux on the bottom wall is presented in Fig. 6 which shows that the present results are in good agreement with the blocked-off FVM of

reference [4]. However, the solution obtained by the blocked-off treatment is shown to produce some error compared with the exact solution as the Cartesian grid cannot exactly conform in shape to the inner circle and the semicircle.

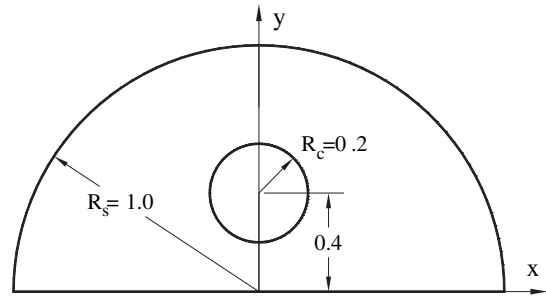


Fig. 5. Schematic of semicircular enclosure with inner circle.

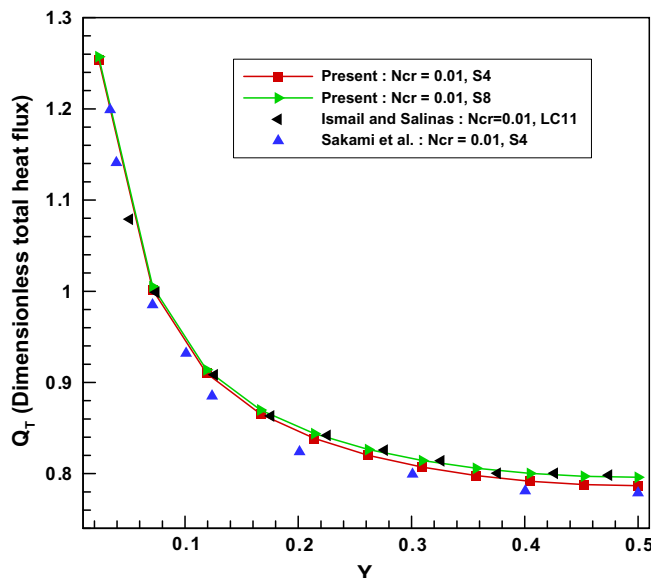


Fig. 4. Dimensionless total heat flux distribution on the hot wall ( $X = 0$ ) of square enclosure for  $N_{CR} = 0.01$ .

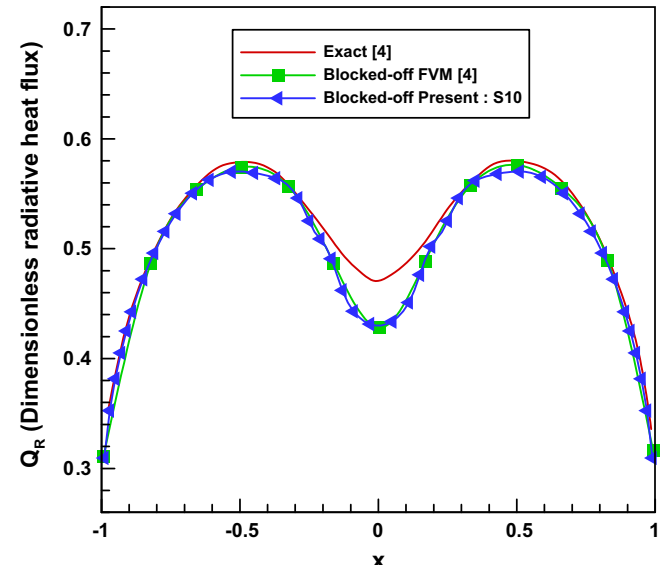


Fig. 6. Radiative heat flux distribution over the bottom wall in a semicircular enclosure.

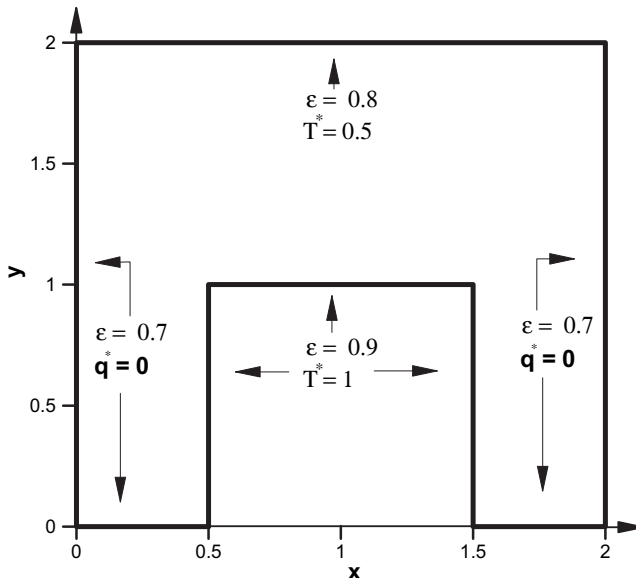


Fig. 7. Geometry, wall properties and boundary conditions of Test problem 1.

## 8. Results

### 8.1. Test problem 1

The first test deals with the combined conductive–radiative heat transfer in the enclosure shown in Fig. 7. In this problem, we investigate the effect of various influencing parameters, such as the extinction coefficient, conduction–radiation parameter, scattering albedo and anisotropic scattering on the top wall ( $y = 2$ ) heat flux. The effects of these parameters have been given in the following sections. The wall properties and the boundary conditions also are shown in Fig. 7. For all the cases, we have considered  $S_6$  angular mesh and  $N_x \times N_y = 40 \times 40$  spatial mesh.

#### 8.1.1. Extinction coefficient ( $\beta$ )

Fig. 8 shows the effect of the extinction coefficient on the total heat flux and the radiative heat flux fraction  $\eta$  (fraction of radiative heat flux to total heat flux) over the top wall when the enclosure contains an isotropic scattering medium with  $N_{CR} = 0.01$  and  $\omega = 0.5$ . The rise in the extinction coefficient has been contributed to the rise in both the absorption coefficient and the scattering coefficient in a proportional manner as  $N_{CR}$  and  $\omega$  remain constant.

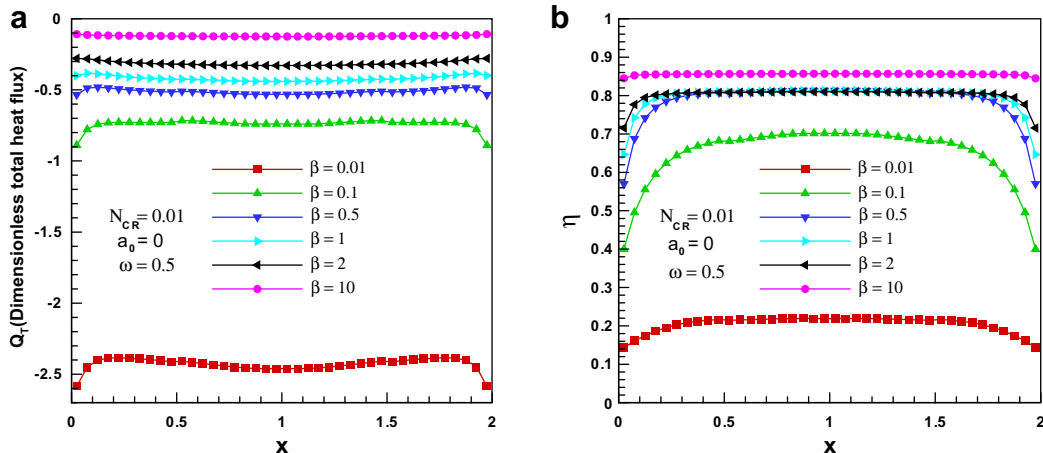


Fig. 8. The effect of extinction coefficient (a) on the total heat flux and (b) on the radiative heat flux fraction along the top wall.

Fig. 8(b) shows that increasing  $\beta$  makes the radiation to become the dominant mode of heat transfer. The rise in the extinction coefficient when  $N_{CR}$  is constant (according to  $N_{CR} = k\beta/(4\sigma T_{ref}^3)$ ), decreases the thermal conductivity,  $k$ . Therefore, the absolute conductive heat transfer value is reduced (Fig. 9(a)). Also, as the extinction coefficient increases, the absolute radiative heat flux value decreases (Fig. 9(b)) because it increases the radiative heat resistant by making radiative heat transfer a local phenomenon.

#### 8.1.2. Conduction–radiation parameter ( $N_{CR}$ )

Consider an absorbing-emitting and isotropic scattering medium with  $\beta = 2 \text{ m}^{-1}$  and  $\omega = 0.5$ . Fig. 10(a) shows the dimensionless total heat flux of the top wall for various values of the conduction–radiation parameter when  $T_{ref}$  and  $\beta$  are constant. As the conduction–radiation parameter increases according to  $N_{CR} = k\beta/(4\sigma T_{ref}^3)$ , conductivity increases and conductive thermal resistance decreases, so, the absolute value of total heat flux increases. For points near the high temperature wall, the absolute total heat flux value becomes considerably higher because they have a low conduction resistance. Fig. 10(b) shows the variation of  $\eta$  for various values of  $N_{CR}$ . It shows that conduction become the dominant mode of heat transfer for  $N_{CR} > 1.0$ . Fig. 11 shows the conduction and radiation part of the total heat flux over the top wall. This figure shows that the radiative heat flux fraction and the absolute value of the radiative heat flux decreases as  $N_{CR}$  increases.

#### 8.1.3. Scattering albedo ( $\omega$ )

The rise in the scattering albedo by keeping the extinction coefficient constant implies that increasing the scattering coefficient is accompanied by a decrease in the absorption coefficient. Fig. 12(a) shows the total heat flux along the top wall for various scattering albedo values. The dimensionless total heat flux seems to be sensitive to the scattering albedo but sensitivity to this parameter is not so strong in contrast to the effect of  $N_{CR}$  or  $\beta$ . In the case of pure scattering,  $\omega = 1.0$ , according to Equation (2), divergence of the radiative transfer for the medium vanishes; that is, the energy equation and the radiative transfer equation get uncoupled but they are interlocked through the boundary condition. Fig. 12(b) shows that as the scattering albedo increases, radiative heat flux fraction increases. As the scattering albedo increases, the fraction of radiative heat flux emanated from the hot wall and absorbed by the medium decreases. Thus, the radiative heat flux reaching the top wall increases (Fig. 13(a)). Also, as the scattering albedo increases, the effect of radiative heating of the hot wall on distant points decreases. Thus, the conductive heat flux over the top wall decreases (Fig. 13(b)).

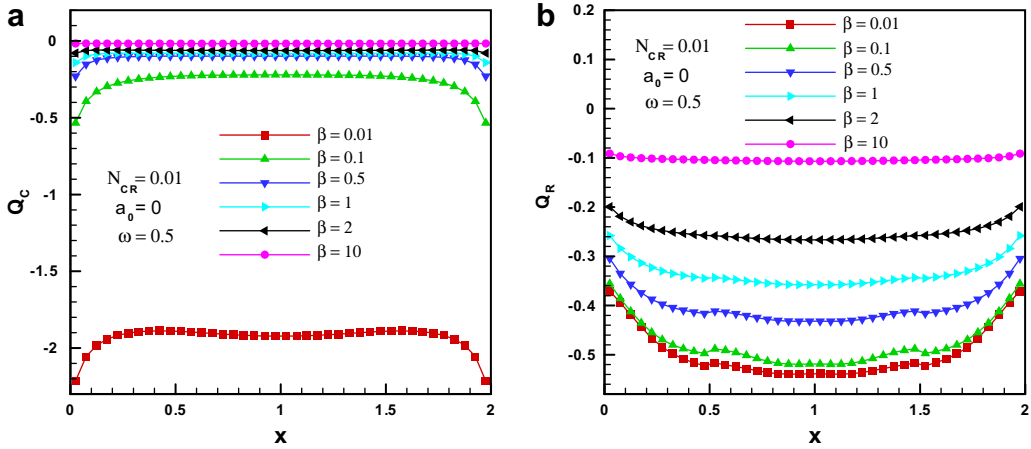


Fig. 9. The effect of extinction coefficient (a) on conductive heat flux over the top wall and (b) on radiative heat flux over the top wall.

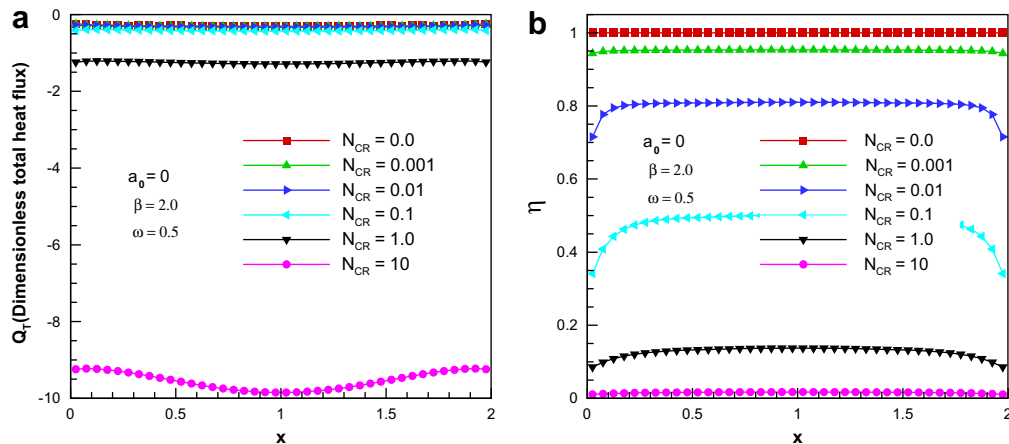


Fig. 10. The effect of conduction–radiation parameter (a) on the total heat flux and (b) on the radiative heat flux fraction along the top wall.

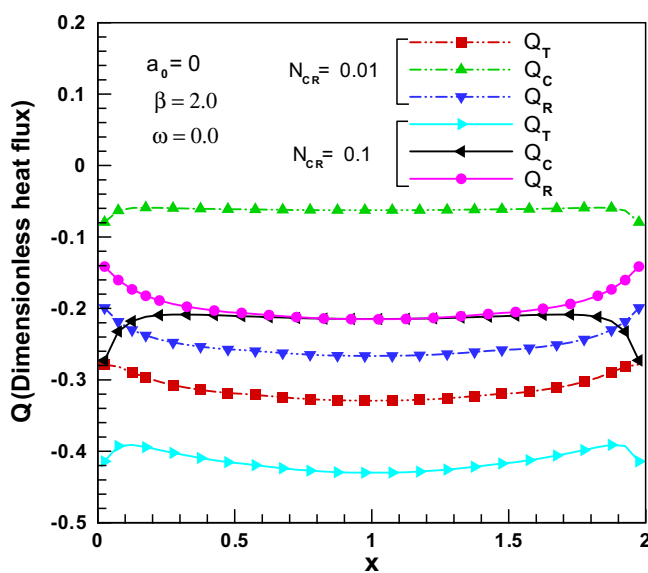


Fig. 11. The effect of conduction–radiation parameter on dimensionless total, conduction part and radiation part of the top wall heat flux.

#### 8.1.4. Anisotropic scattering (asymmetry factor)

The influence of the asymmetry factor is depicted in Fig. 14 where the dimensionless total heat flux and radiative heat flux fraction over the top wall is plotted for  $N_{CR} = 0.001$ ,  $\beta = 2 \text{ m}^{-1}$ ,  $\omega = 0.8$  and different values of the asymmetry factor. It is worth noting that the total heat flux increases as the value of  $a_0$  increases, which means that forward scattering enhances the radiation heat transfer. So, it increases the absolute total heat flux value. It must be mentioned that as these figures show, the effect of the asymmetry factor on the total heat flux and radiative heat fraction is low.

#### 8.2. Test problem 2

For the second problem, we consider the combined conductive–radiative heat transfer in a semicircular enclosure with an internal circle with diffusive and black walls. Figs. 5 and 15 show the geometry and boundary conditions of the test problem 2, respectively. This problem has been considered to investigate the effect of thermophysical parameters, when the heat flux boundary condition exists as a source of energy input to the enclosure, in contrast to the previous test problem in which a high temperature wall was the source of energy. Since the outer semicircular wall is insulated, the total energy input to the enclosure from the inner

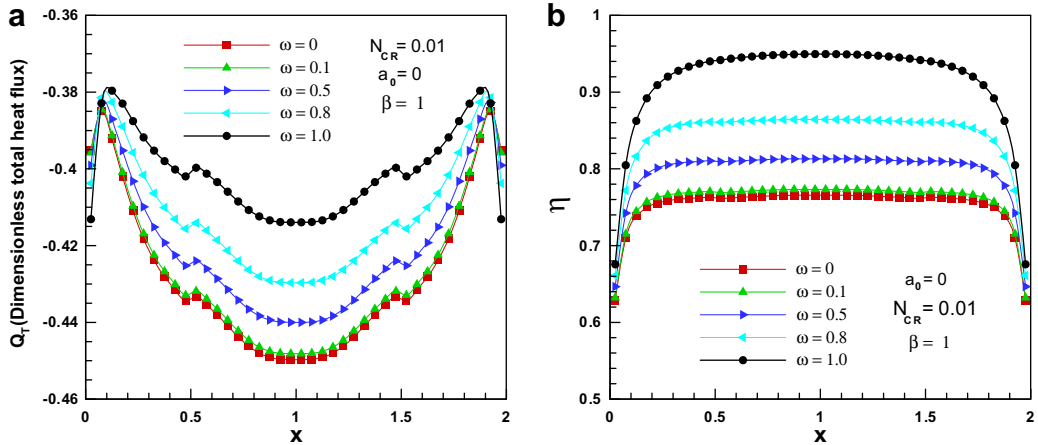


Fig. 12. (a) Dimensionless total heat flux along the top wall and (b) radiative heat flux fraction along the top wall for various values of scattering albedo coefficients.

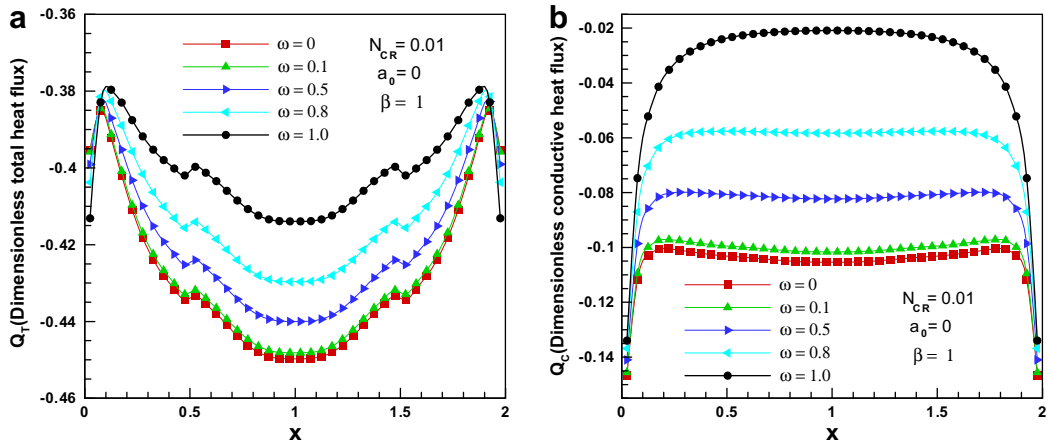


Fig. 13. (a) Dimensionless radiative heat flux and (b) dimensionless conductive heat flux along the top wall for various values of scattering albedo.

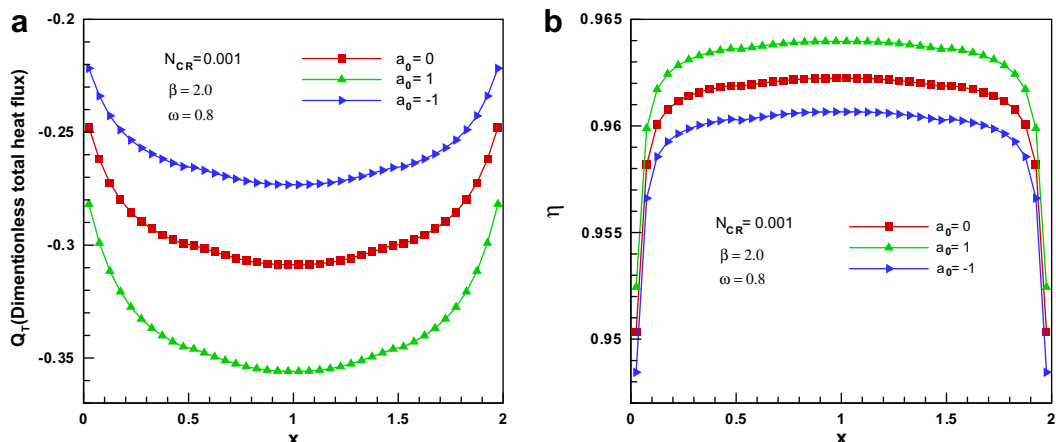


Fig. 14. (a) Dimensionless total heat flux and (b) radiative heat flux fraction along the top wall for various values of asymmetry factor.

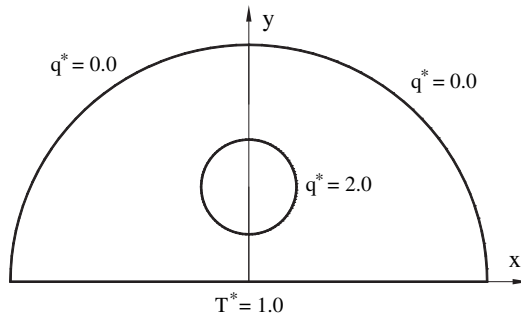


Fig. 15. Boundary conditions of Test problem 2.

circle must leave the bottom wall. Thus, total energy exiting the bottom wall is always constant regardless of medium properties.

#### 8.2.1. Extinction coefficient

Fig. 16 shows the effect of the extinction coefficient on total heat flux and radiative heat flux fraction over the bottom wall. The medium is absorbing-emitting and forward scattering with  $N_{CR} = 0.01$  and  $\omega = 0.5$ . For  $\beta = 0.01$ , conduction is the dominant mode of heat transfer. The absolute value of heat flux attains its maximum in points which are closer to the inner circle. The

absolute value of heat flux decreases in the farther points from the inner circle (these point have higher conductive resistance). As the extinction coefficient increases (conductivity decreases) radiative heat transfer increases. Thus, the absolute value of heat flux in points near the inner circle decreases and it increases for points far from the inner circle. However, when the extinction coefficient further increases, radiation becomes a local phenomenon and the radiation problem converts to a simple conduction problem with a strong temperature dependent conductivity (Rosseland approximation or diffusion approximation [30]). The profile of total heat flux looks like that of the conduction dominant mode of heat transfer.

#### 8.2.2. Conduction–radiation parameter

Fig. 17 shows the effect of the conduction–radiation parameter on the total heat flux and radiative heat flux fraction along the bottom wall. The medium is absorbing-emitting and isotropic scattering with  $\beta = 1 \text{ m}^{-1}$  and  $\omega = 0.5$ . As  $N_{CR}$  increases, conductive heat transfer becomes the dominant mode of heat transfer.

#### 8.2.3. Scattering albedo ( $\omega$ )

Fig. 18 shows the dimensionless total heat flux and radiative heat flux fraction along the bottom wall for various values of scattering albedo. As Fig. 18(a) shows, the dimensionless total heat flux seems to be less affected by variations in scattering albedo.

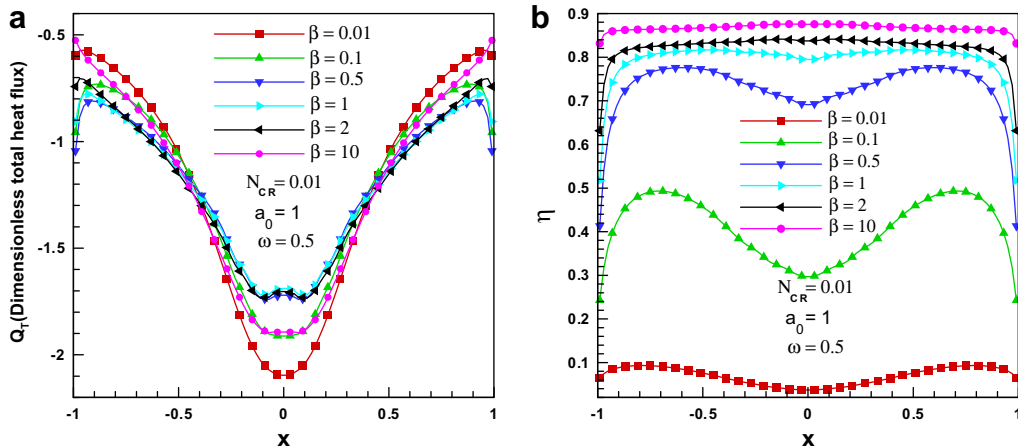


Fig. 16. The effect of extinction coefficient (a) on the total heat flux and (b) on the radiative heat flux fraction along the bottom wall.

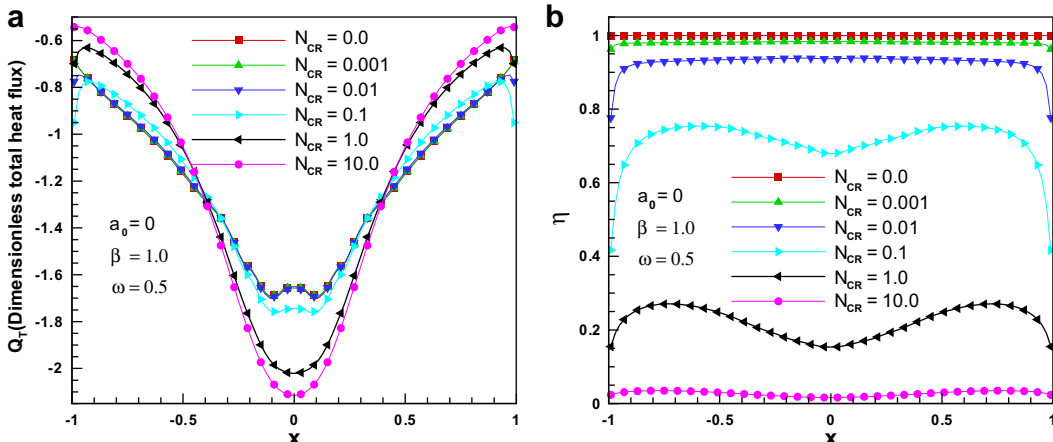


Fig. 17. (a) Dimensionless total heat flux and (b) radiative heat flux fraction along the bottom wall for various values of conduction–radiation parameters.

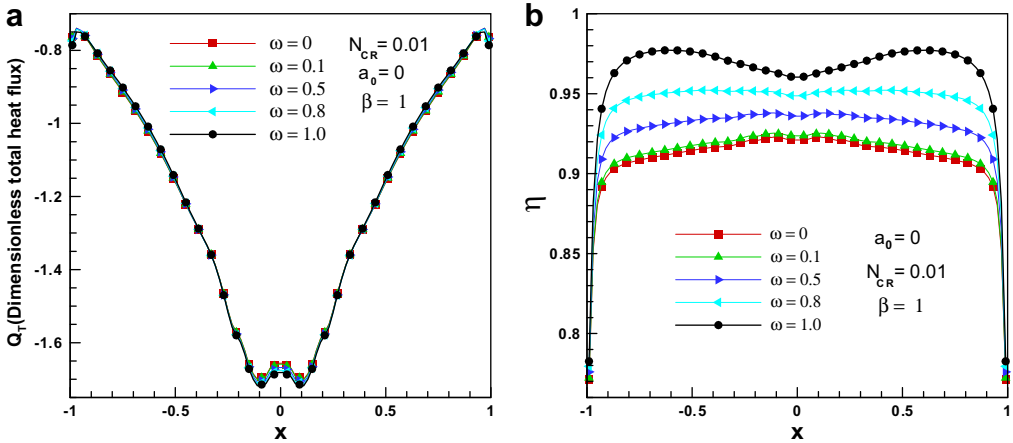


Fig. 18. (a) Dimensionless total heat flux and (b) radiative heat flux fraction along the bottom wall for various values of scattering albedo coefficients.

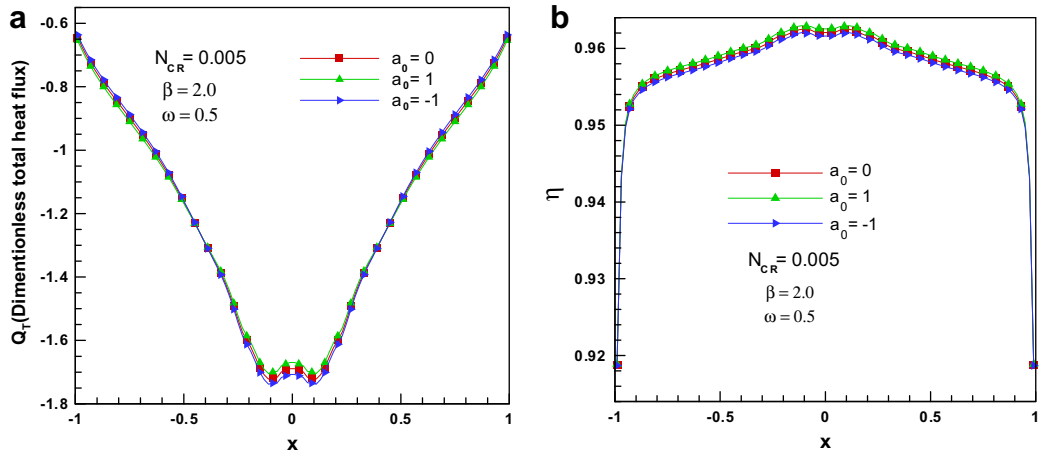


Fig. 19. (a) Dimensionless total heat flux and (b) radiative heat flux fraction along the bottom wall for various values of the asymmetry factor.

However, the radiative heat flux fraction changes due to variations in scattering albedo.

#### 8.2.4. Anisotropic scattering (asymmetry factor)

The effect of the asymmetry factor on the total heat flux and radiative heat flux fraction along the bottom wall is shown in Fig. 19. Results show that the effect of asymmetry factor is negligibly small in this case.

## 9. Conclusion

The investigation of combined conductive and radiative heat transfer within the irregular geometries with absorbing, emitting, and anisotropic scattering medium has been modeled using the blocked-off method in a Cartesian coordinates system. In the first part of this work, the results of the present method were validated for conduction–radiation in a simple geometry and radiation in irregular geometries. Compared with the benchmarked results, this method gives satisfying predictions.

In the second part, this approach has been applied to analyze the effect of the main thermophysical parameters (conduction–radiation parameter, scattering albedo, and asymmetry factor and extinction coefficient) on the total, conductive and radiative heat flux of the walls. Results show that the magnitude of the ratio of the

radiative heat transfer to the conductive heat transfer should be at least unity ( $N_{CR} \leq 1.0$ ) to require a radiation heat transfer calculation. We have also shown that the most important thermophysical parameters are the conduction–radiation parameter and the extinction coefficient.

The present paper shows that the blocked-off method can be used to model the combined conductive and radiative heat transfer in enclosures with blockage, inclined and curved walls. However, in the case of enclosures with curved walls or skewed boundaries, such as Fig. 5, these boundaries need to be treated in a stepwise fashion and this requires a fine grid to obtain accurate results.

## Appendix A. Dimensionless form of energy equation

The dimensionless form of the energy equation (Equation (1)) is expressed as

$$\frac{\partial^2 \theta}{\partial X^2} + \frac{\partial^2 \theta}{\partial Y^2} = S_R \quad (A1)$$

where,

$$S_R = \frac{(1 - \omega)}{N_{CR}} (\theta^4 - G^*) \quad (A2)$$

The parameters and dimensionless variables are

$$G^* = G / (4\sigma T_{ref}^4) = \sum_{n=1}^M I(\vec{r}, \vec{s}^n) w^n / (4\sigma T_{ref}^4), \quad \theta = T / T_{ref},$$

$$N_{CR} = k\beta / (4\sigma T_{ref}^3), \quad \omega = \sigma_s / \beta, \quad X = \beta x \text{ and } Y = \beta y$$

where  $\omega$  is scattering albedo and  $N_{CR}$  is the conduction–radiation parameter. For Equation (A1), the boundary conditions are

$$\theta(\vec{r}_{w-T}) = \theta_w \quad (A3)$$

$$q_T^*(\vec{r}_{w-F}) = q_{Tw}^* \quad (A4)$$

where  $\vec{r}_{w-T}$  and  $\vec{r}_{w-F}$  are the specified temperature part and specified heat flux part of the boundary condition, respectively. The dimensionless radiative, conductive and total heat fluxes are calculated as follows:

$$q_R^*(\vec{r}_w) = q_R / (\sigma T_{ref}^4) = \sum_{n=1}^M (I(\vec{r}_w, \vec{s}^n) (n_w \cdot \vec{s}^n) w^n) / (\sigma T_{ref}^4) \quad (A5)$$

$$q_c^* = q_c / (\sigma T_{ref}^4) = -4N_{CR}\nabla\theta \quad (A6)$$

$$q_T^*(\vec{r}_w) = q_C^* + q_R^* \quad (A7)$$

where the superscripts  $R$ ,  $C$  and  $T$  are abbreviations for radiation, conduction and total heat flux, respectively.

## References

- [1] A. Sanchez, T.F. Smith, Surface radiation exchange for two dimensional rectangular enclosures using the discrete ordinates method. *J. Heat Transf.* 114 (1992) 465–472.
- [2] J.C. Chai, H.S. Lee, S.V. Patankar, Treatment of irregular geometries using a Cartesian coordinates control angle control volume based discrete ordinate method, in: Proceedings of the International Heat Transfer Conference, Atlanta, American Society of Mechanical Engineers, August 8–11, 1993, pp. 35–43.
- [3] J.C. Chai, H.S. Lee, S.V. Patankar, Treatment of irregular geometries using a Cartesian coordinates finite volume radiation heat transfer procedure. *Numer. Heat Transf. B* 26 (1994) 225–235.
- [4] D.Y. Byun, S.W. Baek, M.Y. Kim, Investigation of radiative heat transfer in complex geometries using blocked-off, multiblock and embedded boundary treatments. *Numer. Heat Transf. A* 43 (2003) 807–825.
- [5] F. Asllanaj, V. Feldheim, P. Lybaert, Solution of radiative heat transfer in 2-D geometries by a modified finite volume method based on a cell vertex scheme using unstructured triangular meshes. *Numer. Heat Transf. B* 51 (2007) 97–119.
- [6] H.P. Tan, M. Lallemand, Transient radiative–conductive heat transfer in flat glasses submitted to temperature, flux and mixed boundary conditions. *Int. J. Heat Mass Transf.* 32 (5) (1989) 795–810.
- [7] H.L. Yi, H.P. Tan, H.C. Zhang, J.F. Luo, Ray-tracing/nodal-analyzing model for transient thermal behavior of a scattering medium with a variable refractive index. *Numer. Heat Transf. A* 49 (2006) 607–634.
- [8] H.L. Yi, M. Xie, H.P. Tan, Transient coupled heat transfer in an anisotropic scattering composite slab with semitransparent surfaces. *Int. J. Heat Mass Transf.* 51 (2008) 5918–5930.
- [9] H.L. Yi, H.C. Zhang, H.P. Tan, Transient radiation and conduction heat transfer inside a plane-parallel participating gray medium with boundaries having different reflecting characteristics. *JQSRT* (2009). doi:10.1016/j.jqsrt.2009.06.003.
- [10] S. Chandrasekhar, *Radiative Transfer*. Clarendon Press, Oxford, 1950.
- [11] K.D. Lathrop, B.G. Carlson, *Discrete Ordinates Angular Quadrature of the Neutron Transport Equation*. Los Alamos Scientific Laboratory, 1965, Technical Information Series Report LASL 3186.
- [12] K.D. Lathrop, Use discrete ordinates methods for solution of photon transport problems. *Nucl. Sci. Energy* 24 (1966) 381–388.
- [13] W.A. Fiveland, Discrete ordinates solutions of the radiative transport equation for rectangular enclosures. *J. Heat Transf.* 106 (1984) 699–706.
- [14] W.A. Fiveland, Three dimensional radiative heat transfer solutions by the discrete ordinates method. *J. Thermophys. Heat Transf.* 2 (4) (1988) 309–316.
- [15] M.A. Ramankutty, A.L. Crosbie, Modified discrete ordinates solution of radiative transfer in two dimensional rectangular enclosures. *J. Quant. Spectrosc. Radiat. Transf.* 57 (1997) 107–140.
- [16] M.A. Ramankutty, A.L. Crosbie, Modified discrete ordinates solution of radiative transfer in three dimensional rectangular enclosures. *J. Quant. Spectrosc. Radiat. Transf.* 60 (1998) 103–134.
- [17] M. Sakami, A. Charette, Application of a modified discrete ordinates method to two dimensional enclosures of irregular geometry. *J. Quant. Spectrosc. Radiat. Transf.* 64 (2000) 275–298.
- [18] W. Yuen, E. Takara, Analysis of combined conductive–radiative heat transfer in a two-dimensional rectangular enclosure with a gray medium. *Trans. ASME J. Heat Transf.* 110 (1988) 468–474.
- [19] T.Y. Kim, S.W. Baek, Analysis of combined conductive and radiative heat transfer in a two-dimensional rectangular enclosure using the discrete ordinates method. *Int. J. Heat Mass Transf.* 34 (1991) 2265–2273.
- [20] K.H. Lee, R. Viskanta, Two-dimensional combined conduction and radiation heat transfer: comparison of the discrete ordinates method and the diffusion approximation methods. *Numer. Heat Transf. A* 39 (2001) 205–225.
- [21] S.C. Mishra, A. Lankadasu, K.N. Beronov, Application of the lattice Boltzmann method for solving the energy equation of a 2-D transient conduction–radiation problem. *Int. J. Heat Mass Transf.* 48 (2005) 3648–3659.
- [22] S.K. Mahapatra, S.B. Mahapatra, Numerical modelling of combined conductive and radiative heat transfer within square enclosure using discrete ordinate method. *J. Heat Mass Transf.* 40 (2004) 533–538.
- [23] S.K. Mahapatra, B.K. Dandapat, A. Sarkar, Analysis of combined conduction and radiation heat transfer in presence of participating medium by the development of hybrid method. *J. Quant. Spectrosc. Radiat. Transf.* 102 (2006) 277–292.
- [24] M. Sakami, A. Charette, V. Le Dez, Application of the discrete ordinates method to combined conductive and radiative heat transfer in two-dimensional complex geometry. *J. Quant. Spectrosc. Radiat. Transf.* 56 (1996) 517–533.
- [25] D.R. Rousse, Numerical predictions of two dimensional conduction, convection and radiation heat transfer – I. Formulation. *Int. J. Therm. Sci.* 39 (2000) 315–331.
- [26] D.R. Rousse, G. Gautier, J.F. Sacadura, Numerical predictions of two dimensional conduction, convection and radiation heat transfer – II. Validation. *Int. J. Therm. Sci.* 39 (2000) 315–331.
- [27] K.A.R. Ismail, C.T.S. Salinas, Gray radiative conductive 2D modeling using discrete ordinates method with multidimensional spatial scheme and non-uniform grid. *Int. J. Therm. Sci.* 45 (2006) 706–715.
- [28] F. Asllanaj, G. Parent, G. Jeandel, Transient radiation and conduction heat transfer in a gray absorbing-emitting medium applied on two dimensional complex shaped domains. *Numer. Heat Transf. B* 52 (2007) 179–200.
- [29] J.F. Luo, X. Shen, Numerical method of the ray tracing-node analyzing method for solving 2-D transient coupled heat transfer in a rectangular semi-transparent medium. *Numer. Heat Transf. A* 55 (2009) 465–486.
- [30] M.F. Modest, *Radiative Heat Transfer*, Second ed., 2003.
- [31] K.D. Lathrop, Spatial differencing the transport equation: positivity vs. accuracy. *J. Comput. Phys.* 4 (1969) 475–498.
- [32] S.V. Patankar, *Numerical Heat Transfer and Fluid Flow*. McGrawHill, New York, 1980.